Hindawi
Journal of Nanomaterials
Volume 2021, Article ID 8132868, 10 pages
https://doi.org/10.1155/2021/8132868

Research Article

Preparation, Characteristics, and Controlled Release Efficiency of the Novel PCL-PEG/EM Rod Micelles

Huiling Song,[1] **Yu Yin**,[1] **Jiahui Peng**,[1] **Zixiu Du**,[1] **and Wei Bao**[2]

[1]*School of Pharmacy, Shanghai Jiao Tong University, 800 Dongchuan Road, Shanghai 200240, China*
[2]*Department of Obstetrics and Gynecology, Shanghai General Hospital Affiliated with Shanghai Jiao Tong University, Shanghai, China, No. 100, Haining Road, Shanghai 200080, China*

Correspondence should be addressed to Wei Bao; forever_chipper@hotmail.com

Received 14 June 2021; Revised 2 November 2021; Accepted 26 November 2021; Published 29 December 2021

Academic Editor: Ilker S. Bayer

In order to achieve sustained and controlled release of the hydrophobic cargoes, improve the bioavailability, and reduce the side effects of antibiotics, the model drug erythromycin (EM) was used to prepare polycaprolactone-polyethylene glycol (PCL-PEG)/EM micelles. PCL-PEG, a biocompatible and biodegradable amphiphilic polymer, was used as carrier material of micelles to optimize the formulation and preparation process by orthogonal design. The morphology, stability, drug loading, and encapsulation efficiency and the *in vitro* release behavior of the micelles were investigated. In addition, activity assays of anti-Staphylococcus aureus were performed. The results indicated that PCL-PEG/EM were rod-like micelles with an average particle size of 220 ± 2.6 nm and a zeta potential of +19 mV. The average drug loading and encapsulation efficiency were approximately 6.5% and 97.0%, respectively. The micelles were stable in the serum within three days. At the effective concentration of the drug, the formulation indicated no apparent toxicity to the cells. The micelles were able to rapidly enter *Staphylococcus aureus* (*S. aureus*) and to provide sustained release cargoes that effectively inhibited *S. aureus* proliferation. The present study provided a new platform for the rational and effective use of hydrophobic antibiotics to treat infections.

1. Introduction

Macrolide antibiotics have a broad antibacterial spectrum, mainly by inhibiting the synthesis of bacterial proteins that possess antibacterial roles. These compounds exhibit apparent antibacterial effects on a variety of Gram-positive, Gram-negative, and anaerobic bacteria [1]. Notably, these antibiotics are very effective against legionella and various mycoplasma and chlamydia infections [2, 3]. At present, macrolide antibiotics, which are antibacterial drugs, account for a considerable proportion in clinical medicine. However, at the same time, it is found that this type of antibiotics for bacterial infections will encounter problems, such as poor water solubility and low concentration of lesions, potent toxic, side effects, and microbial resistance [4–6]. The aforementioned shortcomings severely restrict the effective use of antibacterial drugs and cause unnecessary damage to the human body. Simultaneously, side effects, such as bacterial resistance and drug-resistant bacterial infections, will occur [7, 8]. In order to overcome the aforementioned shortcomings of the antibiotics, improve the bioavailability of drugs in the body, reduce the dosage of antibiotics, and avoid bacterial resistance and infection of drug-resistant bacteria, an increased number of effective antibiotic drugs are constantly being developed, while substantial effort has been made on improving their safe and efficient delivery in the body. Among them, the nanodelivery system constructed by polymer biomaterials is still in its infancy in the delivery of antibiotics. However, it has already demonstrated its unique advantages.

Erythromycin (EM) is a broad-spectrum macrolide antibiotic with alkalinity and lipophilicity. EM has a potent antibacterial effect on Gram-positive bacteria, such as *S. aureus*, *Streptococcus pneumoniae*, *Corynebacterium diphtheria*, and *Clostridium bacillus*, as well as on some of Gram-negative bacteria and on mycoplasma [9]. EM has been widely used in the clinical treatment of respiratory infections since it is the primary choice for the treatment of mycoplasma,

pneumonia, and legionella [10, 11]. Since EM is easily absorbed by the gastrointestinal tract following oral administration, it is widely distributed in the body, making it difficult to maintain an effective dose. In addition to the common adverse effects, such as nausea and abdominal pain, EM increases the potential of gastrointestinal side effects, since it is a motilin receptor agonist [12]. EM lactobionate, the commercially available EM injection, increases the drug solubilization in an aqueous solution through the formation of noncovalent bonds between lactobionic acid and EM [13]. However, its effective and complete encapsulation is difficult. Therefore, the nonspecific binding of EM to the normal cell in the blood circulation can easily cause side effects, such as diarrhea, nausea, vomiting, mid-upper abdominal pain, tongue pain, hypogastric appetite, and liver dysfunction, of which the incidence is significantly dose related.

With the rapid development of nanotechnology, the efficiency of drug delivery has been greatly improved. One of the research hotspots of nanoformulations is the targeted treatment of cancer. The research on the nanopreparation of the antibiotic drugs is still in its initial stage. In fact, the structure of the inflammatory tissue becomes looser in the majority of the cases, which facilitates the infiltration of particles in the nanoscale. Several hydrophobic antibiotics can be assembled into nanoformulations to achieve safe and efficient delivery in the body [14], which can increase the drug concentration in the lesions when the same dose is administered. So far, certain EM-imprinted nanoparticles formed by conjugation of EM with polymers have been reported [15]. For example, Bosjnakovic et al. reported on polymer-based dendrimer nanoparticles carrying EM, which was conjugated via ester bonds, whereas Henrik et al. synthesized EM-imprinted poly(methacrylic acid–co–trimethylolpropane trimethacrylate) nanocarriers [16], of which the majority were spherical. In addition, rod-shaped nanoparticles can enter the cells more easily than spherical particles [17]. It was reported that the paclitaxel concentration of rod-shaped micelles in the peripheral blood was rapidly decreased and entered into the main tissues while the blood concentration of TAXOL® was decreased more slowly than that of paclitaxel-containing worm-like micelles [18]. These findings were in sharp contrast to the patterns of spherical paclitaxel micelles, which consistently indicated slower elimination from the peripheral blood compared with that of TAXOL® [19].

Among the various nanoparticle carriers used in biomedical science, poly(caprolactone)-poly(ethylene glycol) (PCL-PEG) is a new material of biodegradable amphiphilic polymers [20], which can form a shell-core structure in the aqueous phase through self-assembly. The inner core consists of the hydrophobic segment polycaprolactone, while the shell is made up of polyethylene glycol. The inner core, which is easy to crystallize, can be used as an ideal compartment for poorly soluble drugs [21]. The shell, which is hydrophilic, can avoid recognition by the reticuloendothelial system and achieve long-term circulation in the body. As micelles can significantly improve the metabolic kinetics of the drug and achieve controlled release, they have received widespread attention in recent years [22]. PCL-PEG is a drug carrier, which has shown optimal stability in the blood circulation due to the low critical micelle concentration (CMC) [23]. Several reports have demonstrated the ability of the PCL-PEG micelles to wrap hydrophobic drugs for *in vivo* delivery [18, 24, 25]. However, no reports have been published on the PCL-PEG/EM micelles. To develop a stable and long-acting EM injection preparation that reduces local drug side effects, PCL-PEG was selected as a carrier material to prepare EM-loaded micelles. Its related antibacterial properties were investigated *in vitro*.

2. Materials and Methods

2.1. Materials. Materials used are as follows: Infinite M200PRO Multimode Microplate Readers (TECAN) FZ-A Hybridization Oven (Taicang Hualida Laboratory Equipment Co., Ltd.), Magnetic Stirring Apparatus (Shanghai Sile Instrument Co., Ltd.), KQ-400KDB Ultrasonic Cleaning Machine (Kunshan Ultrasonic Instruments Co., Ltd.), UPH-I-5TN Ultrapure Water System(Sichuan Ulupure Technology Co., Ltd.), LGJ-10D Freeze dryer (Beijing Sihuan Scientific Instrument Factory), carbon film-coated grids (Electron Microscopy China), PCL_{5000}-PEG2000 and PCL_{2000}-$MPEG_{2000}$ (Xi'an Ruixi Biological Tech. Co., Ltd., 5000 or 2000 is referred to the average molecular weight of the polymer), EM (Beijing Innochem technology Co., Ltd.), Alizarin Red (Shanghai Olbase Biotechnology Co., Ltd.), phosphotungstic acid (Shanghai Macklin Biochemical Technology Co., Ltd.), SKBR-3 cell line (Shanghai Institute of Cell biology, CAS), fetal bovine serum, RPMI-1640 culture medium (Gibco), penicillin-streptomycin solution (100x), and trypsin solution (Thermo Fisher Scientific-China), WST Cytotoxicity test kit, (Shanghai Beyotime Biological Tech. Co., Ltd.), acetone, tetrahydrofuran (THF),*S. aureus*: ATCC 25923, LB liquid culture medium (g/L), tryptone 10 g, yeast extract fermentation 5 g, NaCl 10 g, and pH 7.4.

2.2. Methods

2.2.1. Preparation of EM-Loaded Micelles. EM-loaded micelles were prepared by the solvent-evaporation method as described in our previous method [18]. Briefly, 20, 50, 60, and 100 mg PCL_{5000}-$MPEG_{2000}$ were mixed with 80, 50, 40, and 0 mg of PCL_{2000}-$MPEG_{2000}$ and 7 mg EM powder in 5 mL tetrahydrofuran followed by one-minute sonication (Table 1). Subsequently, distilled water was added to the polymer solutions at a rate of 1 drop every 10 s with vigorous stirring. The addition of water was continued until the water content reached 20-30%, depending on the composition of the block copolymers. The resulting solutions were transferred to dialysis tubes (MWCO = 3500) and dialyzed against double-distilled water to remove the organic solvent THF at room temperature. The EM-containing micelle solution was obtained by removal of nonencapsulated EM using a 0.22 μm microporous filter.

2.2.2. Particle Size Distribution and Zeta Potential. The particle size and zeta potential of blank micelles and EM-loaded micelles were measured by Malvern Nano-ZS90 (Malvern Instruments, Malvern, U.K.) at room temperature. The

Table 1: Formulations for micelle preparation.

Weight ratios of PCL_{2000}-$MPEG_{2000}$ (%)	PCL_{5000}-$MPEG_{2000}$ (mg)	PCL_{2000}-$MPEG_{2000}$ (mg)	EM (mg)
80	20	80	7
50	50	50	7
30	60	40	7
0	100	0	7

particle size distribution was characterized by the intensity averaged particle size and polydispersity index (PdI).

2.2.3. Transmission Electron Microscopy (TEM). The sample was prepared by the 1% phosphotungstic acid negative staining method. The appropriate amount of sample (material concentration = 1 mg/mL) solution was dropped on the carbon film copper mesh at room temperature, and the excess solution was removed with filter paper following one minute of incubation. A small amount of 1% phosphotungstic acid solution was added for negative staining. The solution was allowed to stand for one minute, and the excess solution was removed with filter paper. The copper mesh was naturally dried, and the morphology of the nanoparticles was observed under the TEM (Tecnai G2 spirit Biotwin Biological transmission electron microscopy, FEI Company).

2.2.4. Micelle Stability. The prepared micellar solution with fetal bovine serum (FBS) was mixed in a volume ratio of 1 : 1 and incubated at 37°C in a hybridization oven. The hybridization oven is ideal equipment for modern laboratories to adopt molecular hybridization and can replace plastic hybridization bags and water bath shakers. It can control the temperature accurately and carry out rolling rotation. In order to ensure constant temperature conditions and simulate the movement of the blood in the body, the hybridization oven was used in place of the ordinary shaker to perform the study. The particle size and PdI of the samples were measured by Malvern particle size analyzer at 0, 1, 2, 3, 4, 12, 24, 48, and 72 h, respectively.

2.2.5. Determination of Drug Loading and In Vitro Release. In the current study, a UV spectrophotometric method was established for the determination of the EM content. According to the reports and preexperimental results of UV scanning, EM exhibited a maximum absorption at 209 nm, whereas the carrier material PCL-PEG caused interference [26]. It was found that alizarin and EM could react to generate a 1 : 1 charge-transfer complex, which exhibited maximum absorption at 530 nm with no interference from carrier material. Therefore, 530 nm was selected as the measurement wavelength.

(1) Establishment of EM Determination Method. For the establishment of the standard curve, a total of 5 mg EM was accurately weighed and placed in a 5 mL volumetric flask. The sample was dissolved and diluted to scale with acetone. The EM acetone stock solution of 1 mg/mL was prepared following shaking. A total of 50 mg alizarin was added into a 50 mL volumetric flask and dissolved and diluted with deionized water to 50 mL. The solution was subsequently shaken to obtain a 1 mg/mL alizarin solution. A total of 50, 100, 200, 300, 400, and 500 μL EM acetone stock solution was measured and transferred into a 5 mL volumetric flask. A total of 2 mL acetone solution was used for dilution of 2 mL alizarin solution (1 mg/mL). The final solution was made up to a certain volume with deionized water (the final concentration of EM was 10, 20, 40, 60, 80, and 100 μg/mL). The solution was allowed to stand for 30 min at room temperature, and different concentrations of EM were determined at 530 nm. The absorption value of each concentration was measured 6 times in parallel. A linear regression was calculated based on the absorption value (A) and the EM concentration (C).

For precision, according to the aforementioned method, the absorption values of EM at high, medium, and low concentrations (100, 60, and 10 μg/mL) were measured at 530 nm, respectively. Each sample was measured 6 times, and the results were recorded. The relative standard deviation (RSD) of the calculated concentration was analyzed.

For recovery, a total of 5 mg carrier material PCL_{5000}-PEG_{2000} was transferred to a 5 mL volumetric flask and was dissolved with acetone. The final volume was made up to 5 mL, and a 1 mg/mL PCL_{5000}-PEG_{2000} solution was obtained. Based on the theoretical drug loading of 7% EM, the drug was mixed with acetone stock solution (1 mg/mL) to prepare the EM solution of high, medium, and low concentrations (100, 60, and 10 μg/mL), respectively. The sample was measured at 530 nm, and the results were used to construct a standard curve and obtain the calculated concentration. The recovery can be obtained by calculating the ratio of the calculated concentration and the theoretical concentration of EM.

(2) Determination of Drug Loading (DL), Encapsulation Efficiency (EE), and In Vitro Release. Three batches of EM-containing micelles were prepared based on the optimized formula and process. Each of these contained 3 mg PCL_{5000}-PEG_{2000} and 0.21 mg EM, filtered through a 0.22 μm microporous filter and lyophilized. The weight of each lyophilized sample powder was accurately weighed and dissolved completely with 2 mL acetone, followed by addition of 2 mL of alizarin (1 mg/mL) aqueous solution. The volume was adjusted to 5 mL with water. The optical absorbance of the solution was measured at 530 nm following incubation for 30 min at room temperature. The EM concentration was calculated according to the standard curve. The results were input into the following formula for calculation as follows:

$$\text{EE\%} = \frac{\text{Amount of EM in micelles}}{\text{Total amount of EM added}} \times 100,$$
$$\text{DL\%} = \frac{\text{Amount of EM in micelles}}{\text{Total mass of drug-loaded micelles}} \times 100. \quad (1)$$

In the *in vitro* release experiment, 0.1 M phosphate buffer solution (PBS, pH 7.4) was used as the release medium and ultrahigh-performance liquid chromatography-triple quadrupole mass spectrometry (TQ-XS) was used as the detection device (test provided by the Analysis and Testing Center of Shanghai Jiao Tong University). The TQ-XS was performed using the jet stream focusing technology, which not only improves the atomization temperature but also the electric field density, so that the ionization efficiency can be significantly enhanced and the matrix interference can be effectively shielded, which in turn improves the sensitivity of detection [27, 28]. In order to meet the sink conditions in the release experiment, the concentration of EM was set at a low level. Since the concentration of EM in the released medium was too low to be detected using the conventional liquid chromatography method, TQ-XS was selected with considerably higher sensitivity to determine the concentration of EM. The specific steps were as follows: A total of 500 μL micelle solution containing 200 μg EM was mixed with 3.5 mL release medium and transferred into a 10,000 MWCO dialysis tube. The dialysis tube was immersed in an additional 4 mL release medium to perform release experiments at 37°C (100 rpm). A total of 200 μL dialysate was obtained at predetermined time points (0.5, 1, 2, 4, 8, 24, 48, and 72 h), and the medium was replenished with 200 μL fresh preheated release solution. The samples were stored at 4°C for further determination. Subsequently, the samples were diluted with acetone and filtered through a 0.22 μm microporous filter prior to testing. The peak area was recorded to calculate the concentration of EM. By measuring the concentration, it is possible to estimate the quality of the drug which was removed and released in the medium. The cumulative released drug is the sum of the drug contained in the release medium and the removed part. It was calculated according to the following formula (t_n refers to time point at n hours, C_{EM} refers to concentration of EM, A_{EM} refers to amount of EM which was removed in each sampling, and V refers to volume of released medium):

$$A_{\text{EM}}(t_n) = C_{\text{EM}}(t_n) \times 200\,\mu\text{L},$$
$$\text{Cumulative released drug}(t_n) = C_{\text{EM}}(t_n) \times V + A_{\text{EM}}(t_{n-1}) + \cdots + A_{\text{EM}}(t_{0.5}),$$
$$\text{Cumulative release\%}(t_n) = \frac{\text{Cumulative released drug}(t_n)}{A_{\text{total drug}}} \times 100. \quad (2)$$

2.2.6. Cytotoxicity Assay. SKBR-3 breast cancer cells were selected as the cell model to determine the cytotoxicity of the drug by using the WST kit method. The specific process is described as follows: The conventionally cultured SKBR-3 cells were digested with trypsin and counted. The cells (1×10^3/well) were treated in a 96-well plate, and three groups were designed as follows: the EM group, EM micelle group, and blank micelles group. Following 24-hour incubation, the culture solution was replaced by 60 μL of a drug solution diluted with sterile 0.1 M PBS (pH 7.4). The drug concentrations of the EM and the EM micelle groups were 4, 8, 20, 40, and 80 μg/mL, respectively. The blank micellar group contained the same concentration of PCL-PEG, and three replicates were set for each group. Following incubation for 4 h, the serum-free medium containing the drug was replaced with 200 μL fresh medium containing 10% serum. Following 20 h incubation, 20 μL WST reagent was added to each well and the solution was finally incubated at 37°C for 30 min. The absorbance of each well was measured at 450 nm to calculate cell viability.

2.2.7. Uptake of EM-Loaded Micelle by S. aureus. To prepare fluorescent EM micelles, the method described previously (Section 2.2.1) was used. The difference was that coumarin-6 was mixed simultaneously with EM and PCL-PEG. The next steps were the same as described previously and a coumarin-6: PCL – PEG = 1 : 1,000 mass ratio was achieved. In the micelle uptake experiment of *S. aureus*, 1 mL of $OD_{600} = 0.5$ bacterial suspension was placed in a 2 mL tube and subsequently 10 μL fluorescent micelles containing 300 ng coumarin-6 were added. The micelles were replaced with the same volume of PBS in the control group. Subsequently, the bacterial suspension was mixed with the fluorescent micelles and incubated in a 37°C incubator. The uptake was terminated at a specific time point (10 min, 30 min, 1 h, 1.5 h, and 2 h), and the tube was removed from the incubator and centrifuged for 10 min (5,000 rpm/4°C). Subsequently, the supernatant was carefully discarded and the bacteria were resuspended in 1 mL PBS. The process was repeated three times to ensure that the nonencapsulated micelles were completely washed away. Finally, the bacteria were resuspended in 500 μL PBS.

2.2.8. Evaluation of Antibacterial Activity against S. aureus

(1) Preparation of Test Samples with Gradient Concentration. The aforementioned EM-loaded micelles were divided into two parts as follows: one was subjected to minimum bacteriostatic concentration (MIC) test following incubation for 72 h in 0.1 M PBS (pH 7.4) at 37°C and the other was directly subjected to the MIC test. The blank micelles and EM were used as controls. In order to retain the same concentration of materials, the EM-loaded micelle sample was diluted in PBS to 0.32 mg/mL EM and 3 mg/mL PEG-PCL. The procedure for dilution of the test sample solution was as follows: A sterile 96-well plate was used, and 300 μL liquid was obtained into the first well. A total of 150 μL sterile PBS was added to wells 2-8. A total of 150 μL solution was transferred from the first to the second well and mixed well. A total of 150 μL solution from the second well was finally transferred to the third well. This step was repeated until the sixth well, and 150 μL solution was transferred to the seventh well. A total of 150 μL sterile PBS was added as a growth control in the last well. Thereby, a series of gradient concentration test solutions were obtained.

(2) Determination of MIC. The microbroth dilution method recommended by CLSI 2013 was used for determination. A single colony of *S. aureus* was isolated and purified from a solid plate. The colony was mixed with 3 mL Luria-Bertani (LB) liquid culture medium. The resulting solution was cultured overnight at 37°C and diluted with the same liquid culture medium to obtain a bacterial suspension of approximately 10^7 CFU/mL. A sterile 96-well culture plate was used, and 20 μL of the test sample dilution solution was added with different gradient concentrations prepared in accordance with Establishment of EM Determination Method. A total of 180 μL of each bacterial suspension was added. The EM solution and the PCL-PEG material solution (same concentration) were used as controls. Following incubation for 20 h at 37°C, the results were obtained. The effective concentrations of EM used in the preparations were 32, 16, 8, 4, 2, 1, 0.5, 0.25, and 0 μg/mL. The effective concentrations of PCL-PEG were 300, 150, 75, 37.5, 18.75, 9.4, and 0 μg/mL. Three replicates of the same test sample were set up in test. The results of MIC referred to the standard (7.6.3) recommended by the CLSI 2013, and the lowest drug concentration that completely inhibited bacterial growth in the wells was termed MIC. A total of 200 μL bacterial suspension was transferred into a 96-well black plate and the fluorescence intensity was detected at Ex = 466 nm /Em = 504 nm.

3. Results and Discussion

3.1. Optimization of Preparation Methods. According to the preliminary experiment, four related factors that affected the size distribution and stability of micelles were selected as follows: the different ratios of PCL_{2000}-$MPEG_{2000}$ and PCL_{5000}-PEG_{2000}, the drug loading, the temperature of rotary steaming, and the volume of tetrahydrofuran. The results are shown in Tables 2–5. As noted from the tables below, when the mass fraction of PCL_{2000}-PEG_{2000} ranged between 0% and 50%, the drug loading was approximately 5% to 20%, the rotary steam temperature was between 30°C and 40°C, and the volume ratio of tetrahydrofuran to deionized water was 3 : 1 to 5 : 1. Under these conditions, the micelles with optimal stability could be obtained within three days.

According to the results from the single-factor experiments, the L_{16} (4^4) table was selected to design experiments aiming to further optimize the formulation. The following four main factors were included: mass ratio of different carrier materials (*A*), drug loading capacity (*B*), rotary steaming temperature (*C*), and the amount of THF used during the process (*D*). The specific experimental design and results are shown in Tables 6 and 7.

From the results described in Table 7, it can be seen that the factors affecting the drug loading and encapsulation efficiency of EM-loaded micelles can be categorized as $(A) > (B) > (C) > (D)$. Among them, factor (*A*), (*B*), and (*C*) exhibited significant effects, while (*D*) demonstrated the smallest influence. The optimal preparation was A4B1C1D3, that is, to prepare micelles using 100% PCL_{5000}-PEG_{2000} with a theoretical drug loading of 7%, a rotary evaporation temperature of 30°C, and a THF to deionized water volume ratio of 7 : 1 were required. By using this optimal experimental protocol, 3 batches of EM-loaded micelles were prepared and stored at 4°C for subsequent experiments.

In the present study, the titration method was used to prepare EM-loaded poly(caprolactone)-pol (ethylene glycol) micelles, which were formed based on a thermodynamic process. The properties of the carrier material had a large impact on its particle size, morphology, and drug-loading capacity. Generally speaking, the greater the proportion of the hydrophilicity, the smaller the particle size, whereas the larger the hydrophobic portion, the higher the drug-carrying capacity. Therefore, the L_{16} (4^4) orthogonal experiment was used to optimize the drug loading, the ratio of two different types of carrier materials in the prescription (i.e., the ratio of PCL_{2000}-$MPEG_{2000}$ and PCL_{5000}-PEG_{2000}) (Tables 1–6), the rotary steaming temperature and the oil-

Table 2: Single factor results of different mass fractions of PCL_{2000}-$MPEG_{2000}$.

Weight ratios (%)	Size (nm)	PdI[a]	72 h stability
80	133.1	0.299	Poor
50	176.7	0.220	Good
30	182.2	0.222	Good
0	212.5	0.209	Good

[a]Polydispersity index.

Table 3: Single-factor results of different drug loading.

Weight ratios (%)	Size (nm)	PdI[a]	72 h stability
5	171	0.237	Good
10	182.8	0.211	Good
15	187.5	0.260	Good
20	183.6	0.247	Good

[a]Polydispersity index.

Table 4: Single-factor results of different rotary steaming temperatures.

Temperature (°C)	Size (nm)	PdI[a]	72 h stability
30	312.6	0.263	Good
40	304.3	0.271	Good
50	316.7	0.287	Poor
60	368.3	0.213	Very poor

[a]Polydispersity index.

Table 5: Single-factor results of different organic phase/water ratio.

THF/H_2O *V*/*V*	Size (nm)	PdI	72 h stability
1	110.2	0.269	Very poor
3	212.6	0.220	Good
5	209.6	0.216	Good
10	187.4	0.357	Poor

[a]Polydispersity index.

Table 6: The factor level of the orthogonal experimental design.

Levels	Factors			
	Mass fraction[a] (*w*/*w*%) *A*[e]	DL[b] (*w*/*w*%) *B*[e]	Temperature[c] (°C) *C*[e]	Volume ratio[d] (*V*/*V*) *D*[e]
1	50	7	30	3
2	35	10	35	5
3	15	15	40	7
4	0	20	45	9

[a]PCL_{2000}-PEG_{2000}mass fraction, [b]drug loading, [c]rotary steaming temperature, [d]organic phase/water ratio, [e]*A*-*D* are indicated as in Table 7.

Table 7: The results of the orthogonal experimental design.

No.	Factors				Results	
	A[c]	*B*[c]	*C*[c]	*D*[c]	DL[a] (%)	EE[b] (%)
1	1	3	2	4	5.38	35.86
2	1	1	1	1	5.14	73.50
3	1	2	4	3	2.21	22.08
4	1	4	3	2	1.36	6.80
5	2	4	1	4	7.97	39.83
6	2	3	4	2	6.18	41.18
7	2	2	2	1	3.65	36.48
8	2	1	3	3	4.81	68.70
9	3	4	2	3	9.06	45.30
10	3	3	3	1	4.98	33.20
11	3	1	4	4	4.80	68.53
12	3	2	1	2	6.35	63.52
13	4	3	1	3	13.84	88.95
14	4	4	4	1	9.53	47.65
15	4	1	2	2	4.96	70.79
16	4	2	3	4	4.77	47.65
K1	38.08	75.31	74.77	53.53		
K2	52.20	46.68	52.87	50.28		
K3	58.94	57.39	43.07	63.74		
K4	72.03	41.87	50.54	53.69		
R	33.95	33.44	31.7	13.46		

[a]Drug loading, [b]encapsulation efficiency, [c]*A*-*D* are shown as in Table 7.

water ratio during preparation. It has been found by specific experiments that the aforementioned factors exhibited a certain effect on the stability of the micelles.

3.2. Characterization of Micelles

3.2.1. Particle Size Distribution and Morphology of Micelles. The particle size and distribution of blank micelles and EM-containing micelles (EM-loaded micelle) were measured by dynamic light scattering (DLS). The average diameter of the blank micelles was 204.3 ± 2.3 nm, and the polydispersity index (PdI) was 0.159 ± 0.014. The average diameter of the EM-loaded micelles was 220.2 ± 2.6 nm, and PdI was 0.177 ± 0.025. Compared with the blank micelles, the particle size of the drug-loaded micelles increased slightly, and both of them exhibited a uniform size under room temperature (Figure 1). Concomitantly, the zeta potential of blank micelles and drug-loaded micelles were 12.9 mV and 19.0 mV, respectively (Figure 2).

The morphologies of blank micelles and EM-loaded micelles were observed from TEM (Figure 3). The results indicated that the particle size was approximately 20-50 nm. This was mainly related to the hydrophilic shell of the micelles. In the aqueous solution, the hydrophilic chains of the micelles repel each other and are in a dispersed state, while the TEM is tested under dry conditions. This is the reason why the particle size is significantly reduced. In addition, the data of the present study indicated that, unlike the spherical drug-loaded nanoparticles reported in most studies, the morphology of the blank micelles and drug-loaded micelles formed using PCL-PEG at a specific ratio was spherical and rod-shaped, respectively (Figure 3). This could be noted by the fact that when the EM was added, the morphology of the micelle changed from a spheroid to a rod-like structure, which indicated that EM participated in the self-assembly of the micelles. This suggested that the rod-shaped hydrophobic core was assembled by both PCL and EM. Related studies have reported that rod-shaped carriers have higher drug-loaded capacity and better tissue penetration compared with those of spherical structures, which improves efficacy and facilitates drug delivery [29].

3.2.2. The Stability of the Micelles. The stability of EM-loaded micelles is shown in Figure 4. Provided the particle size and PdI of EM-loaded micelles were not significantly changed within three days, the stability of micelles was optimal in 50% FBS at 37°C. The results indicate that the rod-shaped morphology possesses optimal stability and has the potential to achieve effective circulation in the body and target the infection site passively.

3.2.3. Drug Loading and In Vitro Release

(1) Establishment of EM Determination Method. The EM content was determined by assessing the transfer reaction of alizarin via ultraviolet spectrophotometry. This reaction which is mainly affected by solvents exhibits high sensitivity in ethanol solutions. However, since the carrier material used was insoluble in ethanol, acetone with reduced sensitivity was selected as an alternative.

The standard curve equation used was the following: $A = 0.0004C + 0.0008$, $R^2 = 0.9922$. The EM concentration

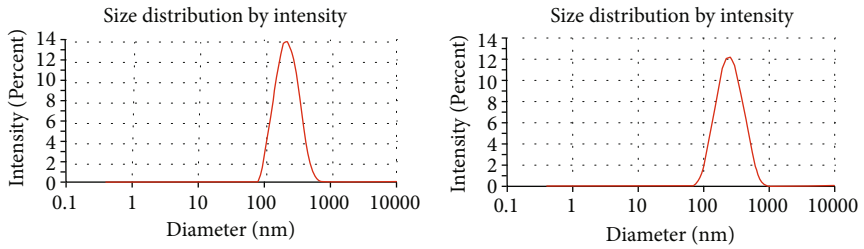

Figure 1: (a) The particle size distribution of blank micelles. (b) The particle size distribution of EM-loaded micelles.

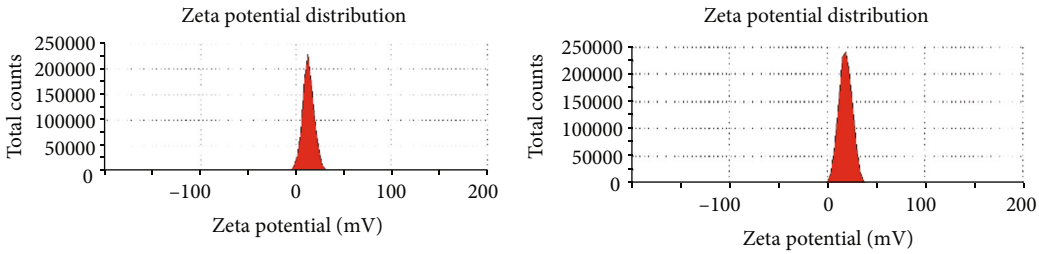

Figure 2: (a) The zeta potential distribution of blank micelles. (b) The zeta potential distribution of EM-loaded micelles.

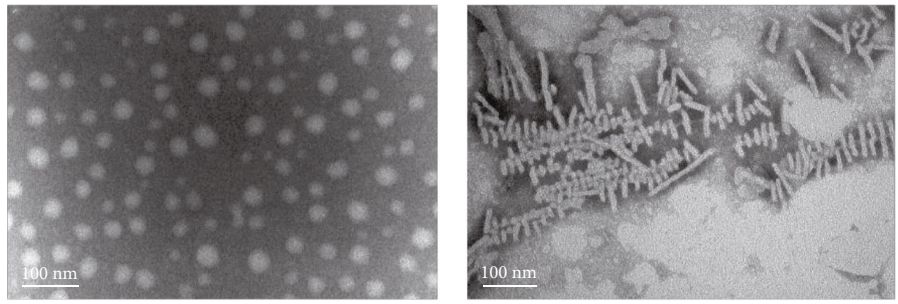

Figure 3: The morphology of (a) blank micelles and (b) EM-loaded micelles observed by TEM.

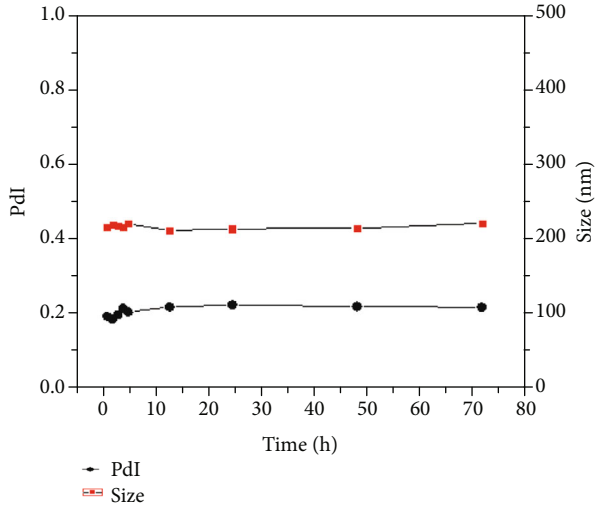

Figure 4: The average size and PdI of EM-loaded micelles in relation to the time of incubation in fetal bovine serum (FBS).

was linear in the range of 10-100 μg/mL. For precision, the calculated RSDs of high, medium, and low concentrations were 1.67%, 2.48%, and 2.40%, respectively. The average recovery of the three different concentrations was equal to 100.2 ± 1.0)%, suggesting that they all met the requirements. This finding indicated that this method exhibited optimal linearity, strong specificity, and optimal reproducibility.

The average drug loading of EM-loaded micelles was 6.48 ± 0.26%, and the average encapsulation efficiency was 92.54 ± 3.82%. The results of the cumulative release rate of EM-loaded micelles at different time points are shown in Figure 5. It can be observed that the EM-loaded micelles exhibited a slow rate of release and that the release ratio reached approximately 80% in three days.

3.3. Cytotoxicity Assay. The cytotoxicity of EM and of the delivering materials is shown in Figure 6. It can be observed that both materials and EM exhibited no toxicity to the cells under

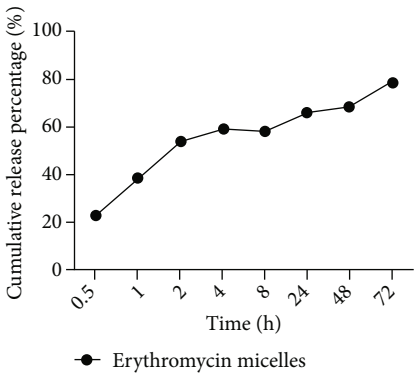

Figure 5: The *in vitro* release of EM from EM-loaded micelles.

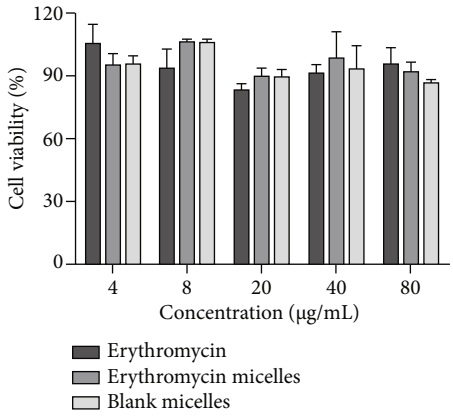

Figure 6: Cytotoxic effects of different concentrations of preparations on SKBR-3 cells.

different drug concentrations. Therefore, it is safe to use PCL-PEG to deliver EM for treatment of bacterial infection.

3.4. In Vitro Uptake of EM Micelles and Antibacterial Activity in S. aureus. As shown in Figure 7, the micelles entered into the *S. aureus* within 10 min. With the extension of the incubation time, the uptake of micelles by the strain was gradually increased and the fluorescence intensity reached saturation within 1 h.

The MIC of the newly prepared drug-loaded micelles was considerably higher than that of the EM. However, following storage of the preparation for three days in a PBS solution with a pH value of 7.4 at 37°C, the bacteriostatic effect on *S. aureus* was comparable to the effect of EM (same concentration), and the carrier material did not show bacteriostatic effects (Table 8). The results indirectly demonstrated that the EM-loaded micelles achieved a slow and controlled drug release, which was also consistent with the results of the *in vitro* release of EM-loaded micelles. This nanoformulation can be applied for the burns on the outside of the body to prevent bacterial infection when EM-loaded micelles are wrapped in the hydrogel.

The aforementioned preliminary *in vitro* experiments demonstrated that the EM rod-shaped nanoformulation could achieve a safe, sustained, and controlled release of EM.

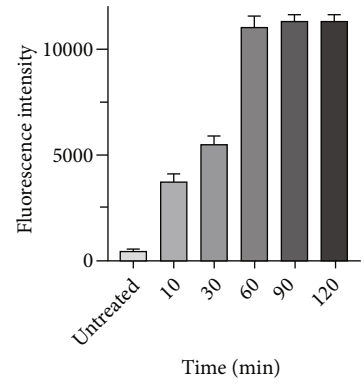

Figure 7: *In vitro* uptake of EM micelles in *S. aureus.*

Table 8: MIC value of test sample against Staphylococcus aureus (μg/mL).

	EM-loaded micelles[a]	EM	PCL-PEG micelle
MIC (0 h)	>32	1	>300
MIC (72 h)	2	1	>300

[a]Recorded based on effective concentration of EM.

Currently, no reports on PCL-PEG/EM micelles have been published. Therefore, this is the first study that examined the loading of EM with PCL-PEG. Firstly, PCL is easy to crystallize. Due to its inner core, it showed a lower CMC (critical micelle concentration), which is more stable during the blood circulation and can be used as an ideal compartment for poorly soluble drugs. Secondly, it is reported that rod-shaped nanoparticles can enter cells and tissues more easily than spherical particles. The data of the present study demonstrated that the morphology of the micelle was changed from a spheroid to a rod-like structure when EM was added, which indicated that EM participated in the self-assembly of micelles. It is well known that the structure of inflammatory tissues becomes looser in the majority of the cases, which facilitates the infiltration of particles in the nanoscale. Therefore, based on these two points, our rod-shaped micelles can exhibit strong tissue and cell penetration abilities. In addition, several reports have been published regarding the ability of PCL-PEG micelles to wrap hydrophobic drugs for successful *in vivo* delivery. The PCL-PEG/EM micelles are not only stable and safe but also show strong penetration and efficient delivery.

4. Conclusions

In the present study, EM-containing PEG-PCL rod-shaped micelles were successfully established, which exhibited an average drug loading of 6.48 ± 0.26% and an average encapsulation efficiency of 92.54 ± 3.82%. The results indicated optimal sustained-release properties and anti-*S. aureus* activity. The current study provides novel insight into the continuous delivery of antibiotics and highlights the potential for the prevention and treatment of burns following wrapping in the hydrogels.

Data Availability

The data used to support the findings of this study are included within the article, and it is also available from the corresponding author upon request.

Conflicts of Interest

The content or the manuscript has not been published or being considered to be published in any other journals. There is no conflict of interest to disclose.

Acknowledgments

This work was supported by the National Natural Science Foundation of China (Nos. 82073802 and 81690262), the Engineering and Medical Cooperation Projects of Shanghai Jiao Tong University (No. YG2021QN137), the National Natural Science Foundation of China (No. 81972425), and National Natural Science Foundation of Shanghai (No. 20ZR1444200). The authors thank the Analytical Center of Shanghai Jiao Tong University for TEM.

References

[1] N. Vázquez-Laslop and A. S. Mankin, "How macrolide antibiotics work," *Trends in Biochemical Sciences*, vol. 43, no. 9, pp. 668–684, 2018.

[2] J. D. Williams and A. M. Sefton, "Comparison of macrolide antibiotics," *Journal of Antimicrobial Chemotherapy*, vol. 31, suppl C, pp. 11–26, 1993.

[3] S. Kobuchi, T. Kabata, K. Maeda, Y. Ito, and T. Sakaeda, "Pharmacokinetics of macrolide antibiotics and transport into the interstitial fluid: comparison among Erythromycin, clarithromycin, and azithromycin," *Antibiotics*, vol. 9, no. 4, p. 199, 2020.

[4] Q. Wang, G. Mi, D. Hickey et al., "Azithromycin-loaded respirable microparticles for targeted pulmonary delivery for the treatment of pneumonia," *Biomaterials*, vol. 160, pp. 107–123, 2018.

[5] E. L. Cyphert, J. D. Wallat, J. K. Pokorski, and H. A. von Recum, "Erythromycin modification that improves its acidic stability while optimizing it for local drug delivery," *Antibiotics*, vol. 6, no. 2, p. 11, 2017.

[6] M. Bin-Jumah, S. J. Gilani, M. A. Jahangir et al., "Clarithromycin-loaded ocular chitosan nanoparticle: formulation, optimization, characterization, ocular irritation, and antimicrobial activity," *International Journal of Nanomedicine*, vol. Volume 15, pp. 7861–7875, 2020.

[7] R. Y. Pelgrift and A. J. Friedman, "Nanotechnology as a therapeutic tool to combat microbial resistance," *Advanced Drug Delivery Reviews*, vol. 65, no. 13-14, pp. 1803–1815, 2013.

[8] M. J. Hajipour, K. M. Fromm, A. Akbar Ashkarran et al., "Antibacterial properties of nanoparticles," *Trends in Biotechnology*, vol. 30, no. 10, pp. 499–511, 2012.

[9] K. D. Lenz, K. E. Klosterman, H. Mukundan, and J. Z. Kubicek-Sutherland, "Macrolides: from toxins to therapeutics," *Toxins*, vol. 13, no. 5, p. 347, 2021.

[10] P. C. Lück and M. Steinert, "Pathogenesis, diagnosis and therapy of legionella infections," *Bundesgesundheitsblatt, Gesundheitsforschung, Gesundheitsschutz*, vol. 49, no. 5, pp. 439–449, 2006.

[11] S. Ewig, P. Tuschy, and G. Fätkenheuer, "Diagnosis and treatment of legionella pneumonia," *Pneumologie*, vol. 56, no. 11, pp. 695–703, 2002.

[12] B. L. Carter, J. C. Woodhead, K. J. Cole, and G. Milavetz, "Gastrointestinal side effects with Erythromycin preparations," *Drug Intelligence & Clinical Pharmacy*, vol. 21, no. 9, pp. 734–738, 1987.

[13] J. F. Camilleri, J. C. Deharo, D. Panagidès et al., "Jet intravenous injection of erythromycin lactobionate. A possible cause of the occurrence of crisis in torsade de pointe," *Annales de Cardiologie et D'angeiologie*, vol. 38, no. 10, pp. 657–659, 1989.

[14] R. S. Kalhapure, N. Suleman, C. Mocktar, N. Seedat, and T. Govender, "Nanoengineered drug delivery systems for enhancing antibiotic therapy," *Journal of Pharmaceutical Sciences*, vol. 104, no. 3, pp. 872–905, 2015.

[15] A. Bosnjakovic, M. K. Mishra, W. Ren et al., "Poly(amidoamine) dendrimer-erythromycin conjugates for drug delivery to macrophages involved in periprosthetic inflammation," *Nanomedicine*, vol. 7, no. 3, pp. 284–294, 2011.

[16] H. Kempe, A. Parareda Pujolras, and M. Kempe, "Molecularly imprinted polymer nanocarriers for sustained release of Erythromycin," *Pharmaceutical Research*, vol. 32, no. 2, pp. 375–388, 2015.

[17] S. M. Loverde, M. L. Klein, and D. E. Discher, "Nanoparticle shape improves delivery: rational coarse grain molecular dynamics (rCG-MD) of taxol in worm-like PEG-PCL micelles," *Advanced Materials*, vol. 24, no. 28, pp. 3823–3830, 2012.

[18] J. Peng, J. Chen, F. Xie et al., "Herceptin-conjugated paclitaxel loaded PCL-PEG worm-like nanocrystal micelles for the combinatorial treatment of HER2-positive breast cancer," *Biomaterials*, vol. 222, article 119420, 2019.

[19] G. Gu, H. Xia, Q. Hu et al., "PEG-co-PCL nanoparticles modified with MMP-2/9 activatable low molecular weight protamine for enhanced targeted glioblastoma therapy," *Biomaterials*, vol. 34, no. 1, pp. 196–208, 2013.

[20] J. Nicolas, S. Mura, D. Brambilla, N. Mackiewicz, and P. Couvreur, "Design, functionalization strategies and biomedical applications of targeted biodegradable/biocompatible polymer-based nanocarriers for drug delivery," *Chemical Society Reviews*, vol. 42, no. 3, pp. 1147–1235, 2013.

[21] Z.-X. Du, J.-T. Xu, and Z.-Q. Fan, "Micellar morphologies of poly(ε-caprolactone)-b-poly(ethylene oxide) block copolymers in water with a crystalline core," *Macromolecules*, vol. 40, no. 21, pp. 7633–7637, 2007.

[22] L. Zhang, Y. He, M. Yu, and C. Song, "Paclitaxel-loaded polymeric nanoparticles based on PCL-PEG-PCL: Preparation, *in vitro* and *in vivo* evaluation," *Journal of Controlled Release*, vol. 152, Suppl 1, pp. e114–e116, 2011.

[23] Q. Wang, J. Jiang, W. Chen, H. Jiang, Z. Zhang, and X. Sun, "Targeted delivery of low-dose dexamethasone using PCL-PEG micelles for effective treatment of rheumatoid arthritis," *Journal of Controlled Release*, vol. 230, pp. 64–72, 2016.

[24] S. M. E. Kamrani and F. Hadizadeh, "A coarse-grain MD (molecular dynamic) simulation of PCL-PEG and PLA-PEG aggregation as a computational model for prediction of the drug-loading efficacy of doxorubicin," *Journal of Biomolecular Structure & Dynamics*, vol. 37, no. 16, pp. 4215–4221, 2019.

[25] Y. Liu, Y. Liu, Z. Du et al., "Skin microbiota analysis-inspired development of novel anti-infectives," *Microbiome*, vol. 8, no. 1, p. 85, 2020.

[26] M. Doostan, H. Maleki, M. Doostan, K. Khoshnevisan, R. Faridi-Majidi, and E. Arkan, "Effective antibacterial electrospun cellulose acetate nanofibrous patches containing chitosan/erythromycin nanoparticles," *International Journal of Biological Macromolecules*, vol. 168, pp. 464–473, 2021.

[27] M. R. Häkkinen, T. Murtola, R. Voutilainen et al., "Simultaneous analysis by LC-MS/MS of 22 ketosteroids with hydroxylamine derivatization and underivatized estradiol from human plasma, serum and prostate tissue," *Journal of Pharmaceutical and Biomedical Analysis*, vol. 164, pp. 642–652, 2019.

[28] N. Scheffe, R. Schreiner, A. Thomann, and P. Findeisen, "Development of a mass spectrometry-based method for quantification of ustekinumab in serum specimens," *Therapeutic Drug Monitoring*, vol. 42, no. 4, pp. 572–577, 2020.

[29] Z. Wang, Z. Chang, M. Lu et al., "Shape-controlled magnetic mesoporous silica nanoparticles for magnetically- mediated suicide gene therapy of hepatocellular carcinoma," *Biomaterials*, vol. 154, pp. 147–157, 2018.